Bull. Nov. Comp. Center, Num. Model. in Atmosph., etc., 7 (2001), 43–58

Notes on pressure gradient correction*

G.A. Platov, John F.F. Middleton

The new pressure gradient correction method was developed for the models with topography-following coordinate system. The test experiments were based on the upwelling and downwelling modeling in Great Australian Bight. They show that new method gives more reliable correction in comparison with Fortunato and Baptista one.

1. Introduction

The topography-following coordinate systems continue to grow in popularity because they are able to provide a better resolution for surface and bottom boundary layers simultaneously. As a matter of fact, one of the most significant disadvantages of the models based on these coordinates is poor approximation of horizontal gradients, especially, in the vicinity of the steep slopes. The development of accurate and efficient numerical methods could be divided [1] into the following four categories: the vertical interpolation method (back to z levels), subtract reference state, high order numerical schemes and retaining integral properties.

In the vicinity of a steep slope, the grid cells are vertically stretched so that the neighboring point in the cross-shore direction at the same level goes much deeper than the nearest point at the underlying sigma-level. It makes the so-called "hydrostatic inconsistency". In fact, if we want a grid to be hydrostatically consistent, then we have to choose the horizontal spacing according to the following constraint

$$\frac{\Delta x}{H}\frac{\partial H}{\partial x} \leq \frac{\Delta \sigma}{\sigma}.$$

If in order to resolve the bottom boundary layer we have at least 1 m resolution near the bottom at 500 m isobath, and the total depth varies from 40 m to 4000–6000 m, then at least 2300–2500 grid nodes are in need to obey this constraint and to build up a simple monotonic deepening.

Let us look at what we will have if, for example, some variable ϕ has a two-layer vertical structure, so that in the area over the solid line a (Figure 1) it is equal to ϕ_1 and in the underlying area – to ϕ_2. The horizontal gradient

*This research was funded as part of the Great Australian Bight circulation project by the Australian Research Council Grant A39700800.

at the point A, which is in the middle of the cell, could be estimated as follows:

$$\frac{1}{2}\left(\frac{\phi_{i,k-1}-\phi_{i-1,k-1}+\phi_{i,k}-\phi_{i-1,k}}{x_i-x_{i-1}}\right)- \frac{\sigma}{2H}\frac{\partial H}{\partial x_*}\left(\frac{\phi_{i,k-1}-\phi_{i,k}+\phi_{i-1,k-1}-\phi_{i-1,k}}{\sigma_{k-1}-\sigma_k}\right),$$

where i and k are indices of X and σ-coordinate grid spacings.

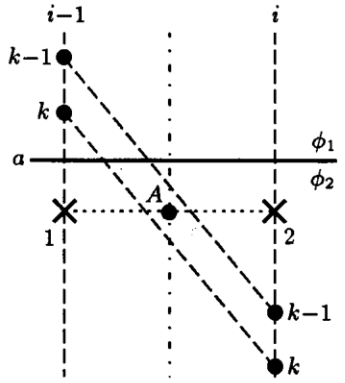

Figure 1. Explanation drawing: the two-layer field of a variable ϕ with the boundary going along the line a, the upper layer has a variable value ϕ_1, while the lower layer has ϕ_2, the problem is to estimate the horizontal gradient at A if a numerical cell is stretched in a way shown in the plot

According to the above assumptions the second term in the expression is equal to zero, because both $\phi_{i,k-1}-\phi_{i,k}$ and $\phi_{i-1,k-1}-\phi_{i-1,k}$ are equal to zero. Both differences in the first term give the same value

$$\phi_{i,k-1}-\phi_{i-1,k-1}=\phi_{i,k}-\phi_{i-1,k}=\phi_2-\phi_1$$

and, finally, the whole expression yields a non-zero value. In other words, it provides a way of converting the originally vertical gradient into the horizontal one. This conversion is as stronger as larger the difference between ϕ_1 and ϕ_2 and as longer the vertical stretching of the grid cell. This example is, of course, idealized. The main point of this idealization is that we consider the transition zone between the two areas to be of zero thickness. In fact it simply means that a depth difference between the two points $(i,k-1)$ and $(i-1,k)$ could be of the same order or larger than thickness of the density interface zone. Thus we might approximately say that the density interface is lying right between $z_{i-1,k}$ and $z_{i,k-1}$.

So, if one has a horizontal interface (or the one which is about to be horizontal) with a large vertical gradient that crosses the steep slope, a large horizontal gradient error is expected when using a numerical cell-based scheme.

2. Back to the Cartesian system

In the situation discussed above, the most effective remedy seams to go back to the Cartesian coordinate system to evaluate the gradient. Looking at Figure 1 one could offer to consider the function values at points 1 and 2 which are at the same level with the point A. These values could be calculated using the vertical interpolation. The following subtraction will give us a horizontal gradient component now evaluated in the Cartesian coordinates. In the previous example, if the vertical resolution is fine enough, meaning that there is, at least, one node present between the solid line and A-level on both vertical lines i and $i-1$, then this would give us a zero gradient value, just what it should be.

Nevertheless, there is still a problem with this approach, when one of two points 1 or 2 is beneath the bottom. So, the value could not be calculated via interpolation (Figure 2). Fortunato and Baptista [2] (hereafter FB) argue also that it is a bad idea to use extrapolation in this case as it can lead to instability in the evaluation of the density and velocity gradients. They proposed to consider point $1'$ instead of point 1, where the value could be estimated using the linear interpolation between the last two points B' and B''. As before the value at point 2 is the linear interpolation between the two nearest grid points Z' and Z''. So, the gradient at A is based on the difference between points 2 and $1'$. Note, that now it is not a central difference scheme and hence we lower the scheme order.

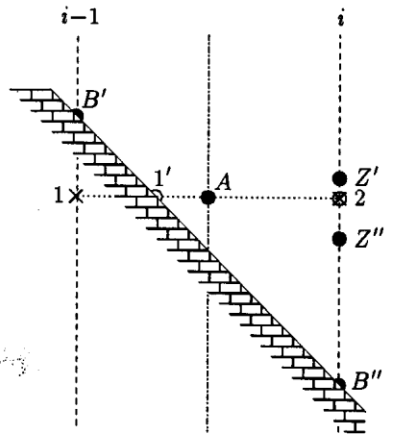

Figure 2. Explanation drawing for the FB method

The practical usage of this approach bring about the idea that the importance of the points B' and B'' is overestimated in this method. The value at point 2 is based on the two nearest grid points Z' and Z'' and the error depends only on the vertical resolution of the grid, while the value of point 1' is based on the points B' and B'' which are strongly separated vertically. So, this value is less reliable in the case of large vertical gradients, just like in the previous example. It makes this scheme closer to the cell-based one. If the line a from the previous example goes horizontally right between the points Z'' and B'', this scheme will give the largest possible gradient value, which is only two times smaller than that in the previous example but again could be significantly different from zero. This situation is quite realistic though, because the vertical scale of the density interfacial zone could be smaller than the depth difference between the points B' and B''.

3. New approach

Keeping the above said in mind, we were trying to build a scheme which instead of interpolating a value across the interface will interpolate the horizontal gradient itself as it does not so dramatically change. The next figure (Figure 3) demonstrates the explanation details.

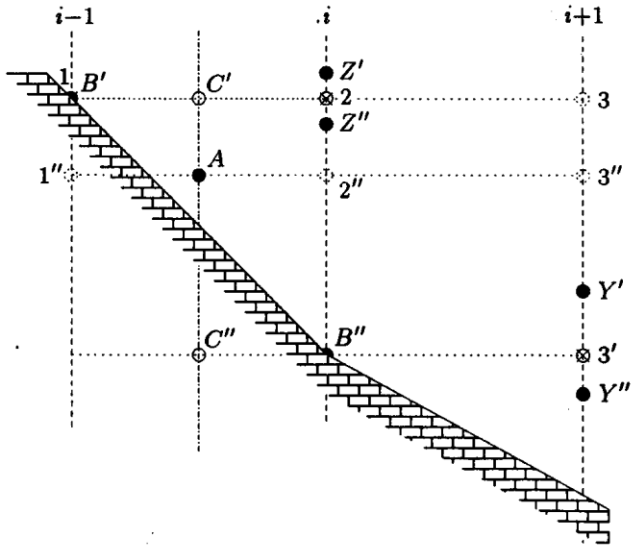

Figure 3. Explanation drawing for the newly proposed method

So, we are going to obtain the horizontal gradient value at the point A using the vertical interpolation of gradients between the points C' and C'', which are at the same level as the points B' and B''. The gradient value at the point C' is calculated via the central difference scheme between points 2 and B'. Like in the previous case the value at 2 is an interpolant between the two nearest grid points Z' and Z''. The gradient value at point C'' is set equal to the gradient value based on the difference scheme between points $3'$ and B'', and $3'$ is interpolant between the two nearest points Y' and Y''. If the depth at $i+1$ is less than at i, then the gradient value at C'' may be set equal to zero.

4. Application technique

So far we were speaking about this problem in general. Now, we will concentrate on the horizontal pressure gradient problem in the Princeton Ocean Model (POM) [3].

The pressure gradient in the Cartesian coordinates is related with the sigma coordinates as follows:

$$\frac{\partial p}{\partial x} = \frac{\partial p_0}{\partial x} + H\int_\sigma^0 \frac{\partial b'}{\partial x}d\sigma',$$

where $b' = b(x, \sigma')$ and

$$\frac{\partial b}{\partial x} = \frac{\partial b_*}{\partial x_*} - \frac{\sigma}{H}\frac{\partial H}{\partial x_*}\frac{\partial b_*}{\partial \sigma},$$

where $*$ is denoted to variables in the sigma coordinates [4]. The buoyancy is $b = (\rho - \overline{\rho})g/\rho_0$, where ρ is density; $\overline{\rho}(z)$ is the horizontally flattened density, and $\overline{\rho}_*(\sigma)$ is its projection on the sigma coordinates; ρ_0 is a constant reference density; g is the gravity constant; $H = H(x)$ is the bottom topography; and $p_0 = p_0(x)$. It is essential to consider $(\rho - \overline{\rho})$ instead of ρ in the buoyancy definition because it helps to subtract interpolation errors caused by transformation from the Cartesian to the sigma coordinates.

Assume, we can evaluate a buoyancy gradient in the Cartesian coordinates using one of the above methods: either the FB or the proposed one. Then the right-hand side of the latter expression may be calculated with the POM standard procedure, which is cell-based, and the numerical scheme is an analogue to the scheme described in our first example. So, it contains an error that can be estimated as

$$\text{error} \approx \epsilon = \left[\frac{\partial b}{\partial x}\right]_{\text{method}} - \left[\frac{\partial b_*}{\partial x_*} - \frac{\sigma}{H}\frac{\partial H}{\partial x_*}\frac{\partial b_*}{\partial \sigma}\right]_{\text{POM}}.$$

After that the obtained ϵ is used as corrector for the POM calculated pressure gradient.

Mellor et al. [4] proposed to evaluate ϵ from the initial conditions and to hold it constant through the whole run. We use three variants: the first is similar to [4], the second with 5 or 10-day-updating period for ϵ with the following 2-day-ramping period, and, finally, with each time-step updating for ϵ (without ramping).

The idea of using two additional variants came after the estimation of the correction changes. It shows that the difference between $\epsilon(t)$ and $\epsilon(t = 0)$ essentially grows up after each 5–10 days, thus needing re-estimation.

5. Preliminary tests

The following preliminary tests strategy was applied.

The prescribed temperature (density) distribution was applied to estimate an error in the pressure gradient evaluation on the basis of the proposed method. The slope in use deepens from 100 m down to 1700 m over 40 km in the offshore direction. In this direction, 9 uniformly distributed grid nodes are used, so that the horizontal spacing is 5 km and deepening between the two neighboring nodes is 200 m. We used 40 sigma levels giving a better resolution for the top and the bottom Ekman layers. The prescribed

density interface intersects the bottom line at the depth h_{int} and goes offshore. A variety of different pressure gradients is produced by a set of the density interface tilts in the offshore direction. They could be identified as upwelling-like, neutral and downwelling-like. The first and the third provide the offshore downward and upward tilts respectively. It means $dh_{\text{int}}/dx < 0$ or > 0. The neutral case assumes no tilt of density interface or $dh_{\text{int}}/dx = 0$. The density interface itself is defined by its thickness d and the magnitude of a temperature drop. We fixed the latter to be 5 degrees assuming that its increasing or decreasing will result in the pressure gradient error linear response. Using this approach we tabulated the maximum pressure gradient error (both positive and negative) depending on the values h_{int}, dh_{int}/dx, and d. It is convenient to represent a pressure gradient error in terms of the geostrophic velocity correction (GVC) made by this error. The results show that a maximum error gives about 58 cm/s artificial bottom current.

In order to decrease pressure gradient error in the Princeton model it is assumed to use the density anomalies $(\rho - \rho_a)$ instead of the density ρ to calculate a pressure gradient. It means that the horizontally averaged density is subtracted from the in situ density giving a smaller vertical density gradient. Analytically it makes no difference for the horizontal pressure gradients until the subtracted density is horizontally constant. We used the tabulated error values to evaluate a maximum possible error in the case of the Great Australian Bight domain grid with initial density distribution. The field of $(\rho - \rho_a)$ at each grid point was considered as a combination of two idealized density interface profiles counteracting with each other. The effectiveness of their counteraction depends on how they overlap each other. There are only three possible cases of their overlapping. The first and most effective is the one when the first interface layer is totally covered with another one. It decreases the magnitude in the density drop in the most effective way. But practically it is not possible to prepare the horizontally constant ρ_a so that it will cover ρ interface everywhere in the region. So, the two other cases take place as well. The second case is when the interfaces are not completely overlapping each other (the density drop is partially decreased) and the third case is when they do not overlap at all (two separate interfaces).

Using this gives us an error histogram collected from all the alongshore nodes where the density interface intersects the bottom line. These histograms will be considered in the next sections.

5.1. General tests

5.1.1. Downwelling tests. We have executed several tests trying to get a better description for pressure gradient in the region of the continental slope in the Great Australian Bight and surrounding area (Figure 4). The

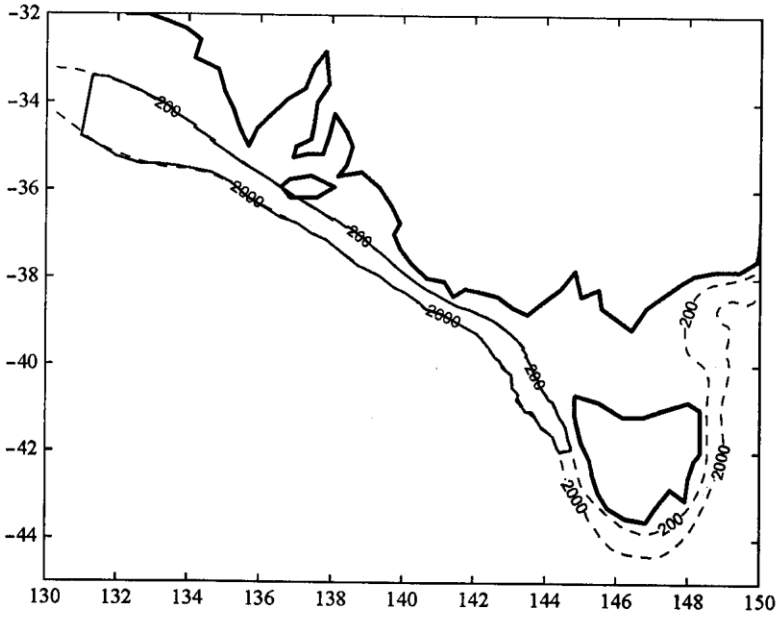

Figure 4. Downwelling model: Part of the Australian shelf slope zone between 200 m and 2 km isobaths used to evaluate the pressure gradient errors for downwelling model domain

OCCAM output data [5] along with [6] and [7] data sets were used to set the initial and the boundary conditions and surface heat, salt and momentum fluxes for the austral winter season. The core of the density interface layer crosses the slope at a depth of 500–600 m, the temperature there being 15–17°C. The interface thickness, estimated as the minimum vertical distance, where the temperature drops by 5°, varies between 200–250 m near the slope, while σ levels deepen here by 80–150 m from point to point in the offshore direction, but near the Kangaroo island and at the Bass Strait west mouth the deepening goes up to 150–200 m. Thus, the ratio here is going down to 1.0–1.7, while all methods give an error less than 10 cm/s only if the ratio exceeds 2.0 value. So, we might expect significant errors in this regions if no average density subtractions were applied.

The first two of the above described histograms present the largest expected errors for the downwelling model domain with the downwelling-like density interface tilt and the neutral tilt. In the downwelling-like case (Figure 5) both methods give more or less reliable results. Even the original POM scheme gives errors less than 5–9 cm/s. In the neutral case, (Figure 6) it is even better, all the methods giving errors less than 3 cm/s, but the FB method and the POM scheme increase the number of points with errors from 7–15 cm/s range.

The first 30 day-run used the ϵ estimated from the initial conditions with

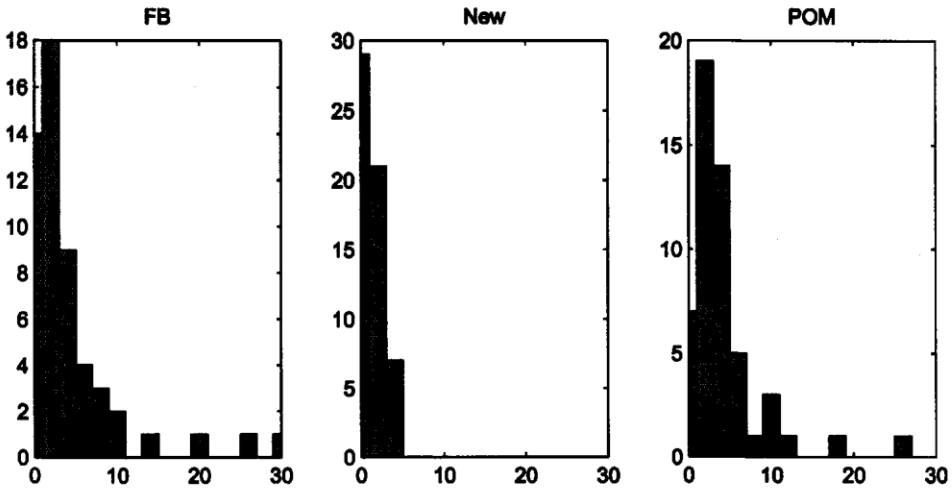

Figure 5. Histogram of a number of points with maximum possible error in specified ranges. Downwelling model – downwelling-like tilt. FB – Fortunato and Baptista, New – the proposed method, POM – the original POM procedure

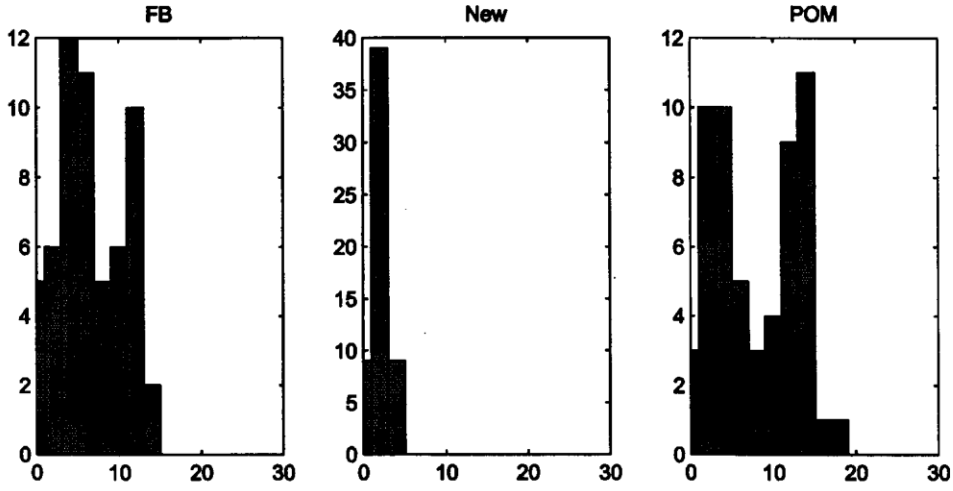

Figure 6. Histogram of a number of points with maximum possible error in specified ranges. Downwelling model – no tilt

the FB approach. The GVC for the specified region has a maximum value about 24 cm/s, while the mean value is slightly below 1 cm/s and r.m.s. value is about 2.4 cm/s. Using the model output we could estimate what might be the correction in the days to follow. The difference $\epsilon(t)-\epsilon(0)$ would give us then the error associated with the pressure gradient inconsistency taking place during the run. Table 1 presents these errors in terms of the associated along-shore component of the geostrophic velocity.

Table 1. Along-shore component of the GVC based on initial density field, errors calculated for days 10, 20 and 30 and GVC based on day 30 density field (test with correction applied one time on day 0)

	Max	Mean	r.m.s.	K.E.
ϵ_0	24.0221	0.9530	2.3892	2.8542
$\epsilon_{10} - \epsilon_0$	8.6146	0.19760	0.52334	0.136940
$\epsilon_{20} - \epsilon_0$	9.0608	0.22361	0.55734	0.155320
$\epsilon_{30} - \epsilon_0$	8.2901	0.23379	0.56001	0.156810
ϵ_{30}	29.8754	1.0018	2.5064	3.1419

Table 2. Along-shore component of the GVC based on initial density field, errors calculated for FB pressure gradient assumption for days 10, 20 and 30 and GVC based on day 30 density field (tests with correction applied once per 10 days)

	Max	Mean	r.m.s.	K.E.
ϵ_0	24.0221	0.9530	2.3892	2.8542
$\epsilon_{10} - \epsilon_0$	8.6146	0.19760	0.52334	0.136940
$\epsilon_{20} - \epsilon_{10}$	8.9601	0.21443	0.52408	0.137330
$\epsilon_{30} - \epsilon_{20}$	10.5024	0.25132	0.63095	0.199050
ϵ_{30}	40.9561	1.0988	2.8177	3.9696

The GVC characteristics grow slightly: the maximum value becomes approximately equal to 30 cm/s, and r.m.s. is about to be the same, i.e., 2.5 cm/s. However the in situ difference becomes significant. Thus, the maximum error is about 8–9 cm/s and the r.m.s. error ranges from 0.52 to 0.56 during the most of the run. We could not get along with 8-9 cm/s error on the slope, because this has the same order as the undercurrent velocity. As we are going to investigate the slope currents, we have to do something to decrease this value. That is why we decided to update the correction term during the run-time. Table 2 shows the result for the FB approach. This method was applied with 10 day interval with the following 2-day linear ramping. We can also estimate the error by subtracting two subsequent correction terms $\epsilon(t_k) - \epsilon(t_{k-1})$. The result becomes even worse. The GVC maximum now grows up to 41 cm/s and the error maximum is 9–10 cm/s. But for this case there is a viewable feature of the two grid point instability in the spatial distribution of basic variables. The mean kinetic energy (divided by density) on the 30th day is equal to 3.35 cm^2/s^2. If the total velocity components were filtered using an analogue of the Shapiro 1-2-1 filter in both i and j directions, then this value would drop to 1.93 cm^2/s^2. It means that 42% of the total kinetic energy contribute to growing in the two-grid-point instability.

At this stage, it is obvious that some sort of filtering must be applied in order to avoid the growth of unrealistic features and to avoid calculations of

Table 3. Along-shore component of the GVC based on initial density field, errors calculated for the FB method for days 10, 20 and, 30 and the GVC based on day 30 density field (tests with correction applied once per 10 days)

	Max	Mean	r.m.s.	K.E.
		Smoothed after run		
ϵ_0	24.0221	0.9530	2.3892	2.8542
$\epsilon_{10} - \epsilon_0$	6.8110	0.19707	0.46502	0.11312
$\epsilon_{20} - \epsilon_{10}$	7.0191	0.25649	0.58259	0.16970
$\epsilon_{30} - \epsilon_{20}$	6.6273	0.25237	0.56379	0.15893
ϵ_{30}	28.7620	1.0041	2.4480	2.9964
		Run-time smoothing		
ϵ_0	24.0221	0.9530	2.3892	2.8542
$\epsilon_{10} - \epsilon_0$	6.8110	0.19707	0.46502	0.11312
$\epsilon_{20} - \epsilon_{10}$	4.3472	0.11170	0.27552	0.03796
$\epsilon_{30} - \epsilon_{20}$	4.6998	0.09218	0.24944	0.03111
ϵ_{30}	29.9252	0.94782	2.3745	2.8190

the pressure gradient correction based on them. In other words we at least have to use the filtered density to calculate the pressure gradient correction. Table 3 demonstrates the result of using the filter described in Appendix in two model runs. The first run is actually the previous one, but the GVC and errors are estimated after the smoothing procedure was applied to the model output density. It leads to dropping the error maximum from 8.6–10.5 cm/s down to 6.6–7 cm/s, while the mean values remain basically the same. The GVC maximum on the 30-th day decreases from 41 cm/s to 29 cm/s, that is, 30% reduction. During the second run, a filter was applied to smooth two grid point waves. It gives a substantial drop of the error maximum from 6.8 to 4.7 cm/s. The mean and the r.m.s. errors become about 2 times smaller by the end of the run and more than 2 times smaller in the comparison with previous run. The advantage of filtering is clear.

5.1.2. Upwelling tests. Like in the previous case, the region used for analysis is a part of the shelf break from 200 m to 2 km close to the most interesting upwelling regions in the Great Australian Bight (Figure 7). The OCCAM output data [5], [6] and [7] data sets were used to set the initial and the boundary conditions and surface heat, salt and momentum fluxes for the austral summer season.

The interface thickness in the upwelling zones off Eyre Peninsula and Bonny Coast is 200–240 m and σ-levels deepening is 120–200 m, providing a ratio value of about 1.0–2.0. It means that even the best correction methods will give an error about 10–15 cm/s without the averaged density subtraction, though it is much better than 40–50 cm/s for the POM scheme.

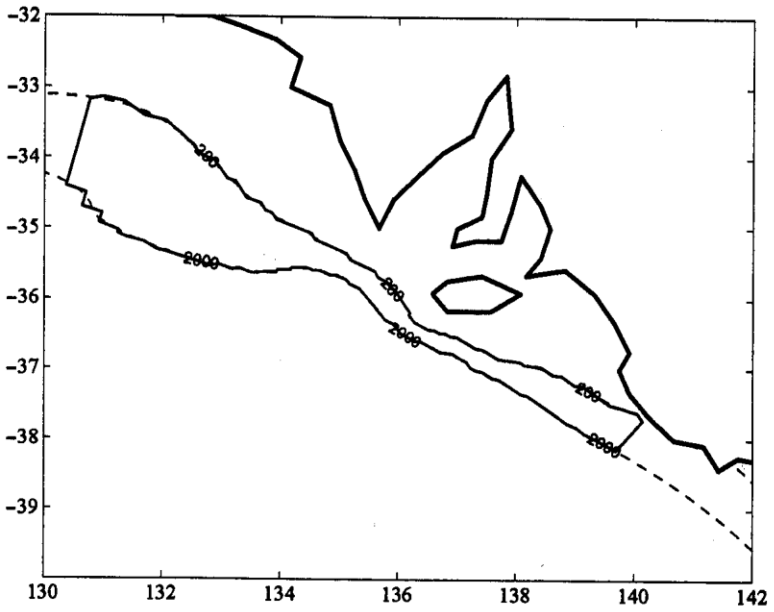

Figure 7. Upwelling model: Part of the Australian shelf slope zone between 200 m and 2 km isobaths used to evaluate the pressure gradient errors for upwelling model domain

The third and the fourth histograms (Figures 8 and 9) demonstrate the results of the largest expected errors for the upwelling model domain with an upwelling-like tilt and the neutral one. In the upwelling-like case (see Figure 8), the error is essentially increasing in comparison with the downwelling cases: the best method is the one proposed here, giving an error for almost all the points less than 9–11 cm/s. The FB method gives a number of points with errors in the 10–20 cm/s range, while the POM scheme upper limit is about 20 cm/s. Nevertheless, the new method continues improvement when moving towards the neutral tilt (see Figure 9) which is a more usual case, they have the error below 3–5 cm/s limit, while the FB and the POM scheme give the increased number of points with errors higher than 5 cm/s.

Table 4 summarizes the results of three subsequent tests with the upwelling model. It shows a progressing improvement from test without any correction applied to test with the FB correction based on the initial density distribution and finally to test with the 10-day updating correction based on the smoothed density distribution. The maximum error during a run reduced from 10.2–10.7 cm/s in the first test to 5.3–6.4 cm/s in the last one, while the mean error on day 30 drops from 0.29753 to 0.0981 cm/s or more than 3 times smaller. The same is for the r.m.s. error. Table 5 shows the same results for the proposed method. The error, when no correction applied, is around 12–15 cm/s, while after the correction based on the initial

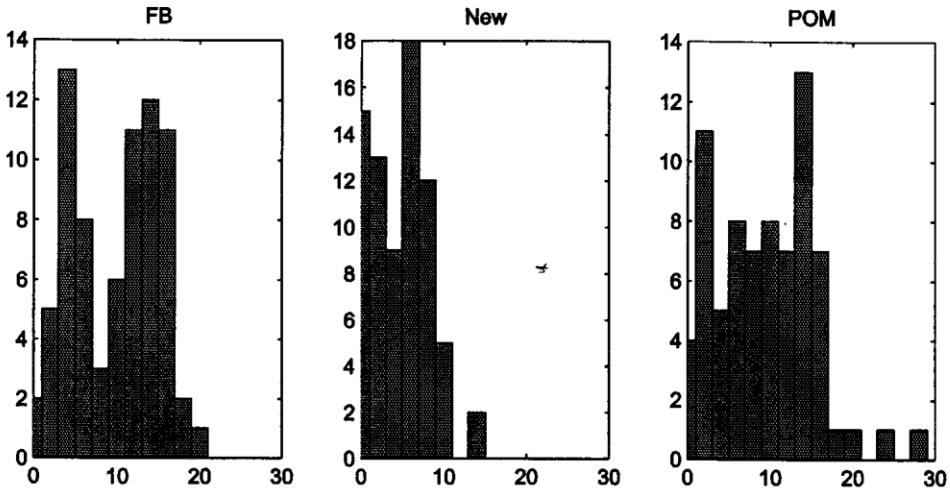

Figure 8. Histogram of a number of points with maximum possible error in specified ranges. Upwelling model – Upwelling-like tilt

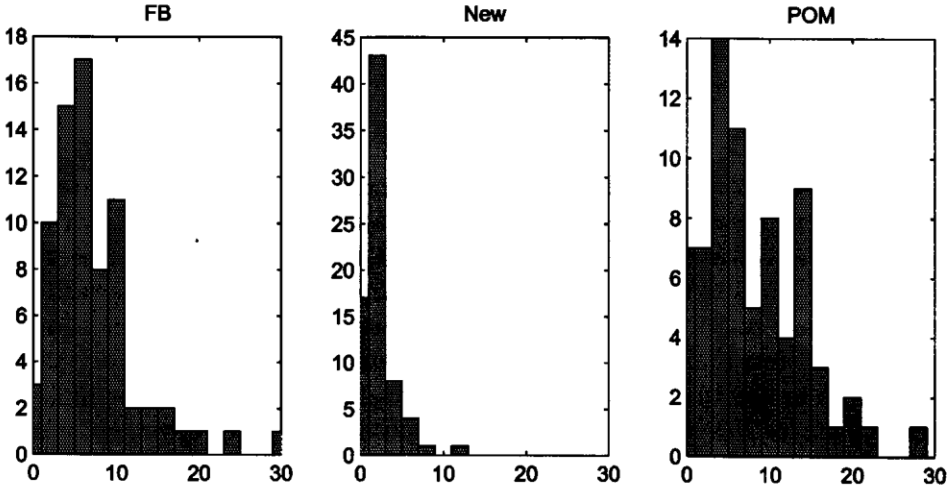

Figure 9. Histogram of a number of points with maximum possible error in specified ranges. Upwelling model – no tilt

density distribution it reduces to 3–3.5 cm/s (2 times smaller than for the FB test) and when correction was applied each 10 days, the maximum error on day 30 was only 1.4 cm/s. The mean and the r.m.s. error values for this method are about 3 times smaller than for the FB.

If one can pre-calculate the vertical interpolation coefficients, then the pressure gradient correction could be calculated on computer much faster. Using this correction for each model time step will reduce the accumulated error associated with updating frequency to zero. Nevertheless, in turn we

Table 4. Along-shore component of the GVC based on initial density field, errors calculated for FB method for days 10, 20, and 30 and the GVC based on day 30 density field

	Max	Mean	r.m.s.	K.E.
ϵ_0	24.0882	0.35847	1.3590	0.92348
Without correction				
ϵ_{10}	10.7438	0.28512	0.89499	0.40050
ϵ_{20}	10.2843	0.28639	0.87444	0.38232
ϵ_{30}	10.2517	0.29753	0.87870	0.38605
With day 0 correction				
$\epsilon_{10} - \epsilon_0$	7.2767	0.12018	0.39359	0.07746
$\epsilon_{20} - \epsilon_0$	7.3433	0.13589	0.40432	0.08174
$\epsilon_{30} - \epsilon_0$	7.2275	0.14796	0.40497	0.08200
ϵ_{30}	21.6669	0.33712	1.1831	0.69988
With correction updated each 10 days				
$\epsilon_{10} - \epsilon_0$	7.2767	0.12018	0.39359	0.07746
$\epsilon_{20} - \epsilon_{10}$	5.3537	0.10842	0.32106	0.05154
$\epsilon_{30} - \epsilon_{20}$	6.2890	0.09810	0.28026	0.03927
ϵ_{30}	23.0209	0.37795	1.2389	0.76743

Table 5. Along-shore component of the GVC based on initial density field, errors calculated for proposed method for days 10, 20, and 30 and the GVC based on day 30 density field

	Max	Mean	r.m.s.	K.E.
ϵ_0	23.3612	0.38109	1.4468	1.04660
Without correction				
ϵ_{10}	12.0430	0.31668	1.02190	0.52216
ϵ_{20}	14.5043	0.34966	1.16520	0.67879
ϵ_{30}	15.2993	0.36772	1.23260	0.75963
With day 0 correction				
$\epsilon_{10} - \epsilon_0$	3.5086	0.04842	0.15399	0.01186
$\epsilon_{20} - \epsilon_0$	3.3775	0.06271	0.15992	0.01279
$\epsilon_{30} - \epsilon_0$	3.2031	0.07484	0.16399	0.01345
ϵ_{30}	21.9998	0.38632	1.3879	0.96315
With correction updated each 10 days				
$\epsilon_{10} - \epsilon_0$	3.5086	0.04842	0.15399	0.01186
$\epsilon_{20} - \epsilon_{10}$	1.7293	0.04221	0.11078	0.00614
$\epsilon_{30} - \epsilon_{20}$	1.4376	0.03129	0.07604	0.00289
ϵ_{30}	19.4960	0.37950	1.3306	0.88524

will have another problem. It is numerical stability. Although a pressure gradient error is high, the POM scheme is numerically well balanced, so it is stable. Each time step the pressure gradient correction will actually substitute new gradients instead of the POM gradients. This could destabilize the numerical integration. For example, when we tried to make use of the FB method at each time step without density smoothing, the model was crashing during the first 10 days of integration.

The analysis shows that the FB method does not cooperate well with the POM model. Right on the slope it gives a number of highs and lows in the along-shore velocity component along with irregular temperature and density distribution. This also leads to a high turbulence activity in this region. We did not try a longer period integration, but it is quite likely that the model could crash under this circumstances if such irregularities grow.

6. Conclusion

According to the analysis done of several pressure gradient correction methods we may recommend how to build a grid to correspond to the density interface layer parameters. The interface thickness and σ-levels deepening ratio seems to be a significant criterion. In case when no average density subtraction applied, most of the methods give an error above 10 cm/s if the ratio is less than 2.1–2.7, while the POM scheme does so if the ratio is below 3.2. This could be substantially improved with the use of this subtraction. But in extreme situations when, for example, the averaged density and the local density interface layers are separated vertically, the error is like we had with two non-interacting interfaces. Thus, the recommendation to make the above-mentioned ratio as large as possible still persists. For both considered downwelling and upwelling models this ratio has a too small value even for regions of strong interest. If the grid had at least the 2 times finer resolution in the region near to 500 m isobath, it would be much better.

Application of a subtracted density allows us to decrease an error in a different way, so that for most of the grid points it would be less than 10 cm/s with the use of a certain appropriate method for the pressure gradient correction.

During the tests it was found that the errors associated with the frequency of correction updating can significantly rise if the correction is seldom applied and density is not smoothed before calculating the correction.

The new approach was developed based on the vertical interpolation of gradients instead of values. The test experiments showed that it gives more reliable correction than any other tested. It is still not clear though, how universal this approach is, and the numerical stability of each time-step usage is the matter of further investigation.

Acknowledgements. We thank Dr. Mauro Cirano for his cooperation in conducting several tests with a downwelling case and for useful discussions on this issue. The results were obtained using the Australian National University Fujitsu VPP300 supercomputer and we thank them for the time made available.

References

[1] Song Y.T. A General pressure gradient formulation for ocean models. Pt. I: Scheme design and diagnostic analysis // Mon. Wea. Rev. – 1998. – Vol. 126. – P. 3213–3230.

[2] Fortunato A.B., Baptista A.M. Evaluation of horizontal gradients in sigma-coordinate shallow water models // Atmos. Ocean. – 1996. – Vol. 34, № 3. – P. 489–514.

[3] Blumberg A.F., Mellor G.L. A description of a three-dimensional coastal ocean circulation model // Three-Dimensional Coastal Ocean Models. Ser. Coastal and Estuarine Series / Ed. N.S. Heaps. – Washington, D.C.: American Geophysical Union, 1987. – Vol. 4. – P. 1–16.

[4] Mellor G.L., Ezer T., Oey L.-Y. The pressure gradient conundrum of sigma coordinate ocean models // J. Atmos. Oceanic Technol. – 1994. – Vol. 11, № 4. – P. 1126–1134.

[5] Webb D., de Cuevas B.A., Coward A.C. The first main run of the OCCAM global ocean model. – Southampton Oceanography Centre, 1998. – Techn. rep. 34.

[6] da Silva A.M., Young C.C., Levitus S. Algorithms and Procedures. Ser. Atlas of Surface Marine Data 1994. NOAA Atlas NESDIS 6. – Washington, D.C.: U.S. Department of Commerce, 1994. – Vol. 1.

[7] Trenberth K.E., Olson J.C., Large W.G. A Global Ocean Wind Stress Climatology Based on ECMWF Analyses. – Boulder, Colorado: Publ. National Center for Atmospheric Research, 1989. – № NCAR/TN-338+STR.

Appendix. Filter smoothing

The original Shapiro filter

$$\tilde{\phi}_i = \frac{\alpha}{2}(\phi_{i-1} + \phi_{i+1}) + (1-\alpha)\phi_i$$

could be considered as a numerical scheme for the one-dimensional diffusion

$$\frac{\tilde{\phi}_i - \phi_i}{\Delta t} = A\frac{\phi_{i+1} - 2\phi_i + \phi_{i-1}}{\Delta x^2},$$

where $\alpha = 2A\Delta t/(\Delta x^2)$. In a more general case, when a grid spacing is not constant, the numerical scheme is to be more complicated. We are going to use the following one:

$$\frac{\tilde{\phi}_i - \phi_i}{\Delta t} = A\frac{2}{x_{i+1} - x_{i-1}}\left(\frac{\phi_{i+1} - \phi_i}{x_{i+1} - x_i} - \frac{\phi_i - \phi_{i-1}}{x_i - x_{i-1}}\right),$$

or

$$\tilde{\phi}_i = \phi_i + A\frac{2\Delta t}{(x_{i+1} - x_i)(x_i - x_{i-1})}\left(\frac{x_{i+1} - x_i}{x_{i+1} - x_{i-1}}\phi_{i-1} + \frac{x_i - x_{i-1}}{x_{i+1} - x_{i-1}}\phi_{i+1} - \phi_i\right).$$

If we set $\alpha = 2A\Delta t/[(x_{i+1} - x_i)(x_i - x_{i-1})]$, then the expression will be analogous to the original one

$$\tilde{\phi}_i = \frac{\alpha}{2}(a\phi_{i-1} + b\phi_{i+1}) + (1 - \alpha)\phi_i,$$

where

$$a = 2\frac{x_{i+1} - x_i}{x_{i+1} - x_{i-1}} \quad \text{and} \quad b = 2\frac{x_i - x_{i-1}}{x_{i+1} - x_{i-1}}.$$

In case of a constant spacing it will give the same form known as the Shapiro filter.

In order to avoid filtering along the constant σ levels, which would lead to additional vertical diffusion, we can use a similar technique like in the case of the pressure gradient correction. To obtain a smoothed value of some variable ϕ at the point (i, k) we can use instead of $\phi_{i-1,k}$ and $\phi_{i+1,k}$ a vertical interpolation yielding the value ϕ at the same depth with $\phi_{i,k}$ on the vertical lines $i - 1$ and $i + 1$. If one of them or both are below the bottom line, then we can set these values equal to $\phi_{i,k}$. This means that we are applying a zero gradient assumption when horizontal lines are crossing the bottom.